NATIONAL TRANSPORTATION SAFETY BOARD

Office of Research and Engineering
Washington, D.C. 20594

June 27, 2014

Aircraft Performance Radar Study

by John O'Callaghan

A. ACCIDENT

Location: Owasso, Oklahoma
Date: Sunday, November 10, 2013
Time: 15:46 Central Standard Time (CST) / 21:46 Coordinated Universal Time (UTC)
Aircraft: Mitsubishi MU-2B-25, registration N856JT
NTSB#: CEN14FA046

B. GROUP

Not Applicable

C. SUMMARY

On November 10, 2013, about 1546 CST[1], a Mitsubishi MU-2B-25 twin-engine airplane, N856JT, impacted wooded terrain while maneuvering near Owasso, Oklahoma. The commercial pilot, who was the sole occupant of the airplane, sustained fatal injuries. The airplane was destroyed. The airplane was registered to Anasazi Winds, LLC, Tulsa, Oklahoma, and was operated by the pilot under the provisions of 14 Code of Federal Regulations Part 91 as a personal flight. Visual meteorological conditions prevailed for the flight, and an instrument flight plan had been filed. The flight departed Salina Regional Airport (KSLN), Salina, Kansas, about 1500, and was en route to Tulsa International Airport (KTUL), Tulsa, Oklahoma.

This *Aircraft Performance Radar Study* presents the results of using Airport Surveillance Radar (ASR) data to calculate the position and orientation (pitch, yaw and roll angles) of the aircraft in the minutes preceding the accident. This information is then used to estimate various performance parameters of interest, including horizontal and vertical speeds, terrain clearance, angle of attack and proximity to stall, and required engine power.

The sections that follow present the radar data used in this *Study*, and describe the methods used to compute the additional performance parameters from this data. The results of these calculations are presented in the Figures and Tables described throughout the *Study*.

[1] All times in this *Study* are in CST based on a 24-hour clock, unless otherwise noted. CST = UTC – 6 hours.

D. DETAILS OF THE INVESTIGATION

I. Radar Data Sources

Description of ARSR and ASR Radar Data

In general, two types of radar are used to provide position and track information, both for aircraft cruising at high altitudes between airport terminal airspaces, and those operating at low altitude and speeds within terminal airspaces.

Air Route Surveillance Radars (ARSRs) are long range (250 nmi) radars used to track aircraft cruising between terminal airspaces. ARSR antennas rotate at 5 to 6 RPM, resulting in a radar return every 10 to 12 seconds. Airport Surveillance Radars (ASRs) are short range (60 nmi) radars used to provide air traffic control services in terminal areas. ASR antennas rotate at about 13 RPM, resulting in a radar return about every 4.6 seconds. The FAA ASR-9 radar at KTUL (TUL) received returns from N856JT starting at about 15:30:13, when the airplane was 60 nmi northwest of the KTUL runway 18L threshold, and descending through 14500 ft. above mean sea level (MSL). The TUL ASR continued to track the airplane throughout its approach to KTUL, including the last minutes of the flight (see Figure 1). Consequently, data from the TUL ASR are used for performance calculations in this *Study*.

Primary and Secondary Radar Returns

A radar detects the position of an object by broadcasting an electronic signal that is reflected by the object and returned to the radar antenna. These reflected signals are called *primary returns.* Knowing the speed of the radar signal and the time interval between when the signal was broadcast and when it was returned, the distance, or range, from the radar antenna to the reflecting object can be determined. Knowing the direction the radar antenna was pointing when the signal was broadcast, the direction (or bearing, or azimuth) from the radar to the object can be determined. Range and azimuth from the radar to the object define the object's position. In general, primary returns are not used to measure the altitude of sensed objects, though some ARSRs do have height estimation capability. ASRs do not have height estimation capabilities.

The strength or quality of the return signal from the object depends on many factors, including the range to the object, the object's size and shape, and atmospheric conditions. In addition, any object in the path of the radar beam can potentially return a signal, and a reflected signal contains no information about the identity of the object that reflected it. These difficulties make distinguishing individual aircraft from each other and other objects (e.g., flocks of birds) based on primary returns alone unreliable and uncertain.

To improve the consistency and reliability of radar returns, aircraft are equipped with transponders that sense beacon interrogator signals broadcast from radar sites, and in turn broadcast a response signal. Thus, even if the radar site is unable to sense a weak reflected signal (primary return), it will sense the response signal broadcast by the transponder and be able to determine the aircraft position. The response signal can also contain additional information, such as the identifying "beacon code" for the aircraft, and the aircraft's pressure altitude (also called "Mode C" altitude). Transponder signals received by the radar site are called *secondary returns*.

N856JT was operating on an instrument flight plan and under instrument flight rules (IFR), and consequently had a discrete transponder beacon code (equal to 4615 in this case) assigned to it (aircraft operating under visual flight rules (VFR) all use a common, VFR transponder code of 1200). From 15:43:37 to 15:44:04, as N856JT was on final approach between 6.1 and 5.1 nmi from the KTUL runway 18L, there is a 27-second gap in the TUL ASR secondary data (corresponding to 5 missing returns). However, during this time, three primary returns consistent with the position of N856JT were received by the TUL ASR. In addition, during this time, the Chelsea / Afton, Oklahoma ATCBI-6 radar[2] (QAF) received secondary returns from N856JT. The QAF secondary returns indicate that the gap in the TUL secondary returns is not due to a problem with N856JT's transponder, but to some other, unknown cause (perhaps a momentary shielding of the transponder antenna on the airplane from the ASR antenna by the fuselage of the airplane itself). The TUL ASR primary returns and the QAF ATCBI-6 returns mentioned here are also shown in Figure 1.

Recorded Radar Data

Recorded data from the TUL ASR and QAF ATCBI-6 were obtained from the FAA, and include the following parameters:

- UTC time of the radar return, in hours, minutes, and seconds. CST = UTC – 6 hours.
- Transponder beacon code associated with the return (secondary returns only)
- Transponder reported altitude in hundreds of feet associated with the return (secondary returns only). The transponder reports pressure altitude. The altitude recorded in the file depends on the site recording the data; some sites record both pressure altitude, and pressure altitude adjusted for altimeter setting (MSL altitude). Others record just the adjusted altitude. The TUL file contains pressure altitude only. The MSL altitude used in this *Study* is set 314 ft. higher than the pressure altitude[3]. The resolution of the altitude data is ± 50 ft.
- Slant Range from the radar antenna to the return, in nmi. The accuracy of this data is ±1/16 nmi or about ± 380 ft.
- Azimuth relative to true or magnetic north from the radar antenna to the return[4]. The azimuth is reported in Azimuth Change Pulses (ACPs). ACP values range from 0 to 4096, where 0 = 0° magnetic and 4096 = 360° magnetic. Thus, the azimuth to the target in degrees would be:

  (Azimuth in degrees) = (360/4096) x (Azimuth in ACPs) = (0.08789) x (Azimuth in ACPs)

  The accuracy of azimuth data is ± 2 ACP or ± 0.176º.
- Latitude and longitude of the radar return. These coordinates are computed by the FAA radar processing systems based on the range and azimuth sensed by the radar. In this *Study,* the recorded latitude and longitude are not used; rather, the airplane position is computed from the recorded range and azimuth, so that the uncertainty in position associated with each return (resulting from the uncertainties in range and azimuth) can

[2] An ATCBI-6 radar is similar to an ARSR, except that it is a beacon-interrogator only (i.e., it can only receive secondary returns, and does not have primary radar capability).

[3] The altimeter setting for the time and location of the accident was 30.26 "Hg, resulting in a pressure altitude about 314 ft. lower than true altitude above Mean Sea Level (MSL).

[4] The TUL ASR records azimuth relative to magnetic north, using a magnetic variation that is nominally 5.97° E. In this *Study*, a variation of 6.03° E is used to make the latitude and longitude computed from the recorded range and azimuth data best match the latitude and longitude coordinates recorded in the file from the FAA. The QAF ATCBI-6 records azimuth relative to true north.

also be computed. The latitude and longitude coordinates computed in this way agree well with the coordinates recorded in the FAA file.

To determine the latitude and longitude of radar returns from the range and azimuth data recorded by the radar, the geographic location of the radar antenna must be known. The coordinates of the TUL ASR antenna are:

36° 12' 45.4756" N latitude; 095° 55' 05.8106" W longitude; elevation 612.8 feet

The coordinates of the QAF ATCBI-6 antenna are:

36° 24' 37.24" N latitude; 095° 26' 10.81" W longitude; elevation 959 feet

Presentation of the Radar Data

To calculate performance parameters from the radar data (such as groundspeed, track angle, pitch and roll angles, etc.), it is convenient to express the position of the airplane in rectangular Cartesian coordinates. The Cartesian coordinate system used in this *Study* is centered on the KTUL runway 18L threshold, and its axes extend east, north, and up from the center of the Earth. The data from the TUL ASR and QAF ATCBI-6 are converted into this coordinate system using the WGS84 ellipsoid model of the Earth.

Figure 1 shows a plan view of the TUL ASR secondary and primary returns, and selected QAF ATCBI-6 returns, for N856JT within 8 nmi north of the KTUL runway 18L threshold. The first TUL ASR return shown on the plot is at 15:42:50, as the airplane is descending through 2500 ft. The plot shows the location of the returns, and the uncertainty boxes surrounding the returns, based on the range and azimuth uncertainty inherent in the data. The uncertainty boxes indicate the area within which N856JT could actually be located at the time of the return, and still be consistent with the possible errors in the range and azimuth sensed by the radar. To reduce unrealistic "noise" in performance calculations, the radar data is "smoothed" using 3rd order B-splines, and the performance calculations use the smoothed data.[5] Note that the limits of the accuracy of the performance calculations should be considered when drawing conclusions based on the calculations. It is generally preferable to regard performance calculations based on smoothed radar data as qualitative indicators of the area of the performance envelope in which an aircraft was operating, rather than as quantitative and precise measurements of performance parameters.

The solid black circles in Figure 1 indicate the smoothed locations of N856JT at the times of the returns (the times are indicated by the black text labels); note that the circles lie within the uncertainty box of each return, as required. The blue text labels indicate the smoothed MSL altitude corresponding to the time of each return. The three primary returns received by the TUL ASR that are consistent with the path of N856JT are shown as the black, open circles. The secondary returns from the QAF ATCBI-6 are shown as the brown, open squares, and the times and MSL altitudes associated with these returns are indicated by the brown text labels. The extended KTUL runway 18L centerline is depicted by the red dash-dot line.

[5] There are other smoothing techniques that can result in a reasonable fit of the raw radar data (i.e., that keep each radar return within its uncertainty box), and each of these will produce slightly different performance calculation results.

The times, contents, and locations of Air Traffic Control (ATC) communications to and from N856JT are shown by the green text labels and red and yellow diamonds. The times and contents of the ATC communications are taken from Reference 1.

The TUL ASR and QAF ATCBI-6 returns plotted in Figure 1 are also listed in Tables 1 and 2.

The north and east coordinates of the raw radar returns, and the curve fits of these returns, are shown as a function of time in Figure 2.

The altitude data for N856JT are presented vs. time in Figure 3, and vs. distance north of the KTUL runway 18L threshold in Figure 4. The ±50 ft. uncertainty bands surrounding the Mode C altitude data are also shown in Figure 3. A curve fit through the altitude data that lies within the Mode C uncertainty bands is also shown in Figures 3 & 4, and is used in the performance calculations presented below.

The radar data presented in Figures 1-4 indicates that at about 15:42:50, N856JT was descending on a southeasterly heading through 2500 ft. MSL about 8 nmi north of the KTUL runway 18L threshold. At about 15:43:00, the airplane leveled off briefly at 2200 ft., and started a right turn towards the runway. The airplane crossed the extended runway centerline at about 15:43:19, and continued the right turn to correct back to the centerline. At about 15:43:25, the airplane resumed its descent, and continued descending until about 15:44:22, when it leveled off at about 1100 ft. MSL (about 400 ft. above ground level (AGL)).[6] The airplane remained at this approximate altitude throughout the remainder of the radar returns. The last return from N856JT received by the TUL ASR was at 15:45:36.4.

As shown in Figure 4, when N856JT leveled off at 2200 ft. MSL at 15:43:00, it was already below the Precision Approach Path Indicator (PAPI) centerline for KTUL runway 18L, and when the airplane resumed its descent at 15:43:25, the PAPI would have displayed 4 red lights, indicating that the airplane was already well below the PAPI centerline.[7]

At about 15:44:00, as N856JT was descending through 1400 ft. MSL, it started a left turn that persisted to the end of the radar data, with the airplane almost completing a full 360° turn. During this turn, the pilot reported to ATC that “I’ve got a control problem”(at 15:44:51) and that “I’ve got a left engine shutdown” (at 15:45:06). The airplane crashed less than 0.05 nmi southwest of the last radar return, about 5 nmi north of the runway threshold, and about 0.05 nmi left (east) of the extended runway centerline.

[6] Terrain elevation data for this *Study* was obtained from the United States Geological Survey (USGS) *National Map Viewer* at http://viewer.nationalmap.gov/viewer/.

[7] The PAPI geometry for KTUL runway 18L was obtained from the FAA’s online database at http://avnwww.jccbi.gov/pls/datasheet_prd/pkg_airport.PRO_SINGLE_RUNWAY?v_air_cntl_num=3025&v_rwy_cntl_num=112741.

II. Estimates of Aircraft Performance Parameters

The radar data defines N856J's position in space as a function of time. The first time derivative of these data define N856JT's velocity relative to the Earth (groundspeed and rate of climb). If the winds aloft are known or estimated, then the airplane's velocity relative to the airmass (i.e., airspeed) can be computed. In addition, given the (known) aerodynamic characteristics of the MU-2B-25 airplane, the orientation (heading, pitch, and roll angles) of N856JT during the flight can also be estimated, assuming that the flight was (1) coordinated (i.e., negligible sideslip angle), and (2) unstalled. Given the pilot's communication to ATC regarding a "control problem" and a "left engine shutdown," it is likely that, because of a potential thrust asymmetry, the sideslip angle was not negligible during the final left turn. If true, this introduces some error into the calculations; even so, the results can be useful and indicative of the general aircraft attitude during the maneuver. In addition, as discussed further below, the calculations indicate that shortly before the end of the radar data, the airplane's lift coefficient (C_L) reached the maximum C_L for the flaps 20 configuration,[8] which suggests that the final descent of the airplane into the ground followed an aerodynamic stall of the wing. However, up to this point, the airplane would have remained unstalled.

Surface wind data for this *Study* are based on the KTUL METAR at 15:53 CST, and winds aloft data are based on upper air soundings from Springfield, MO (KSGF) at 18:00 CST, as provided to the author by an NTSB meteorologist. The METAR reads as follows:

> Weather at KTUL from 1553 CST, wind from 140 degrees at 6 knots, 10 miles visibility, scattered clouds at 9,000 feet agl, air temperature 19 degrees Celsius, dew point temperature 6 degrees Celsius, altimeter setting 30.26 in. Hg. Remarks, sea level pressure 1024.4 hPa, air temperature 19.4 degrees Celsius, dew point temperature 5.6 degrees Celsius.

This surface wind data is merged with the KSGF upper air wind data and plotted in Figure 5.

Aerodynamic data for the MU-2B-25 was provided by Mitsubishi Heavy Industries (MHI) in References 2 - 5. Using loading and empty weight information provided by the NTSB Investigator in Charge (IIC), MHI computed that the weight and center of gravity (CG) of N856JT at landing would have been 8510 lb. and 30.27% mean aerodynamic chord (MAC), respectively. A gross weight of 8510 lb. was used for the calculations in this *Study.*

The position coordinates of the aircraft as a function of time define the aircraft velocity and acceleration components. In coordinated flight, these components lie almost entirely in the plane defined by the aircraft's longitudinal and vertical axes. Furthermore, any change in the *direction* of the aircraft velocity vector is produced by a change in the lift vector, either by increasing the magnitude of the lift (as in a pull-up), or by changing the direction of the lift (as in a banked turn).The lift vector also acts entirely in the aircraft's longitudinal-vertical plane, and is a function of the angle between the aircraft longitudinal axis and the velocity vector (the angle of attack (α)). These facts allow the equations of motion to be simplified to the point that a solution for the airplane orientation can be found given the additional information about wind and the aircraft lift curve.

Figure 6 shows the true airspeed, calibrated airspeed, groundspeed, and rate of climb calculated from the smooth curve fits of the radar data for N856JT and the wind data plotted

[8] Per an email dated 11/19/2013 from the Investigator In Charge (IIC) to the author, evidence in the airplane wreckage indicates that the flaps were extended to 20° and the landing gear were down at the time of impact.

in Figure 5. Note that the speeds based on the unsmoothed radar positions exhibit greater "noisiness" associated with the uncertainty of those positions, and that the speeds based on smoothed positions are less noisy and more realistic. Nonetheless, the results shown in Figure 5 remain an estimate of aircraft speeds rather than an exact, quantitative measurement of the speeds; such an estimate is the best that the resolution and sample rate of the radar data can provide. Figure 6 indicates that the N856JT's airspeed decreased from about 232 KCAS at 15:42:00 to about 95 KCAS at 15:44:12, and then remained between about 90 and 95 KCAS for about 40 seconds. Brief speed oscillations on the order of 5 knots computed on the basis of radar returns, such as those depicted in Figure 6 between 15:44:12 and 15:45:15, must be viewed with caution; the oscillations in question may be the result of uncertainty in position, winds, or a combination of these. However, the calculations suggest that the airspeed remained below 100 KCAS during this time, and perhaps dipped as low as 85 KCAS.

The oscillation in groundspeed and airspeed between 15:45:15 and 15:45:30 must also be viewed with some caution, for similar reasons. Nonetheless, the drop in airspeed to below 80 KCAS shown at 15:45:30, which drives the computed C_L above the maximum C_L for flaps 20 and implies a stall, is consistent with the condition of the wreckage, its location very close to the last radar point, and witness statements.[9]

Some airspeed limitations of interest, taken from Reference 5, are shown in Table 3. Of note, the flaps 20 one-engine-inoperative (OEI) minimum control speed ($V_{MC,20}$) is 93 KCAS. Consequently, the speed data plotted in Figure 6 indicates that N856JT was operating close to $V_{MC,20}$ during the time that the pilot reported control and engine problems.

Figure 7 presents longitudinal performance parameters of interest. The top plot in Figure 7 shows the flight path angle (γ), and the pitch (θ) and angle of attack (α) angles for two configurations: flaps and gear up, and flaps 20, gear down. The stall α for the two configurations, based on information in References 2, 3 and 5, are also shown. The θ and α data for flaps up are shown up until 15:44:18, at which time the computed C_L for this configuration exceeds the corresponding C_{Lmax} (and α exceeds α_{stall}). Similarly, the θ and α data for flaps 20 are shown until 15:45:27. The θ and α data for flaps 20 are shown starting at 15:43:32, corresponding to the time at which the airspeed decreases to 140 KCAS; per Table 3, it is unlikely that the pilot would have deployed the flaps to 20° while the airspeed was above the 140 KCAS flaps 20 flaps extended speed ($V_{FE,20}$).[10]

The bottom plot in Figure 7 shows the computed C_L for flaps up and flaps 20. The data for the two configurations differs only because of thrust effects on the required lift; at flaps 20, the higher drag requires higher thrust, and the component of thrust normal to the flight path vector reduces the lift required from the wing. However, as shown in the Figure, this effect is small. The ranges of data shown for each configuration are clipped in the same way as in the plots of θ and α.

[9] Reference 6 documents one witnesses stating that "the airplane pitched up, stalled, and went into a spiral nose dive" and another stating that "she observed the airplane spiral counter-clockwise straight down toward the ground."

[10] The manufacturer's serial number for N856JT is 306. For this serial number, the flaps 5 extended speed is 175 KCAS; consequently, per Reference 5, the flaps could be deployed to 5° at 175 KCAS or slower.

Figure 7 indicates that the flaps must have been deployed prior to 15:44:18, since the C_{Lmax} for flaps up was exceeded at that time. In addition, the flaps must have been deployed to 20° prior to 15:44:35, when the C_{Lmax} for flaps 5 was exceeded. Furthermore, the flaps were likely deployed to 20° at some time after 15:43:32, in order to respect the 140 KCAS $V_{FE,20}$ limitation. The airplane decelerated below the $V_{FE,5}$ of 175 KCAS at about 15:43:10.

Figure 8 presents the calculation of the roll (ϕ) and heading (ψ) angles. The top plot shows approximately 13° of roll during the right turn between 15:42:55 and 15:43:50 as the airplane maneuvered to line up with the extended runway centerline, and then a roll to the left as the airplane entered its final, left 360° turn. The roll angle required during this left turn is only about 15° to 25°, with the roll angle increasing from about 5° left to 22° left between 15:44:20 and 15:44:30. This increase in roll angle corresponds to the time that the airplane arrested its deceleration and descent and leveled at approximately 95 KCAS and 1100 ft. MSL (see Figures 3 and 6). As discussed below, associated with this level-off is an increase in required horsepower. If the increase in horsepower were only available from one engine, then any thrust asymmetry between the two engines would also be increased, and would increase the rudder deflection (δ_r) and/or sideslip angle (β) required to compensate for the asymmetry. Consequently, the increase in roll angle at this time may reflect these changing parameters affecting the trim of the airplane.

The drag coefficient (C_D) and required horsepower for the flaps up / gear up, flaps 20 / gear down OEI, and flaps 20 / gear up OEI configurations are shown in Figure 9. The airplane's kinetic, potential, and total (kinetic plus potential) energies are also shown. The increase in required horsepower between 15:44:10 and 15:44:30, corresponding to the arrest of the airplane's deceleration and descent described above, is apparent in the second plot. The second plot also shows that large negative horsepower – i.e., additional drag – is required between 15:43:30 and 15:44:00 for the flaps up, gear up configuration, while the horsepower required for the flaps 20, gear down OEI configuration is much closer to zero. This result suggests that the flaps may have been deployed to flaps 20 around 15:43:30, shortly after the time the airplane decelerated below the 140 KCAS $V_{FE,20}$ speed.

The large oscillations in required power between 15:42:30 and 15:43:30 are primarily the result of sudden changes in the computed groundspeed during this time, and the acceleration associated with these changes. Since the abruptness of the changes, and consequent accelerations, are not realistic, neither are the resulting oscillations in required horsepower. Hence, it is appropriate to "filter" these oscillations with the mind's eye, noting that the results indicate a generally low power setting. This conclusion is consistent with the total energy presented in the bottom plot of Figure 9, which reflects a steadily decreasing energy state (and consequently, a low power setting) until about 15:44:10, when the rate of energy decay starts to diminish, and eventually disappears as the airplane maintains a nearly constant total energy state from about 15:44:25 until the end of the data. The reduction in the rate of energy decay corresponds to the increase in required horsepower.

At 15:44:27, the power increases to about the maximum available from one engine under these conditions (about 460 HP, assuming 665 SHP produced by the engine, multiplied by a propeller efficiency (η) of 69% at the corresponding combination of airspeed and altitude).[11] Figure 9 indicates that about 60 HP is required to overcome the drag of the landing gear

[11] In Reference 4, MHI estimates an η of about 69% for an airspeed of 96 KCAS at an altitude of 1300 ft. MSL.

during the level turn at 1100 ft. If the gear had been raised, this power would have been available to increase the airplane's total energy.

E. CONCLUSIONS

This *Aircraft Performance Radar Study* presents the results of using the TUL ASR data to calculate the position and orientation of N856JT in the minutes preceding the accident. The data indicates that at about 15:42:50, N856JT was descending on a southeasterly heading through 2500 ft. MSL about 8 nmi north of the KTUL runway 18L threshold. At about 15:43:00, the airplane leveled off briefly at 2200 ft., and started a right turn towards the runway. The airplane crossed the extended runway centerline at about 15:43:19, and continued the right turn to correct back to the centerline. At about 15:43:25, the airplane resumed its descent, and continued descending until about 15:44:22, when it leveled off at about 1100 ft. MSL (about 400 ft. AGL). The airplane remained at this approximate altitude throughout the remainder of the radar returns.

When N856JT leveled off at 2200 ft. MSL at 15:43:00, it was already below the PAPI centerline for KTUL runway 18L, and when the airplane resumed its descent at 15:43:25, the PAPI would have displayed 4 red lights, indicating that the airplane was already well below the PAPI centerline.

At about 15:44:00, as N856JT was descending through 1400 ft. MSL, it started a left turn that persisted to the end of the radar data, with the airplane almost completing a full 360° turn. During this turn, the pilot reported to ATC that "I've got a control problem"(at 15:44:51) and that "I've got a left engine shutdown" (at 15:45:06). The airplane crashed less than 0.05 nmi southwest of the last radar return, about 5 nmi north of the runway threshold, and about 0.05 nmi left (east) of the extended runway centerline.

The airspeed data presented in this *Study* indicates that N856JT was operating close to $V_{MC,20}$ during the time that the pilot reported control and engine problems. In addition, the calculations indicate that shortly before the end of the radar data, the airplane's C_L reached the maximum C_L for the flaps 20 configuration, which suggests that the final descent of the airplane into the ground followed an aerodynamic stall of the wing. This finding is consistent with the condition of the wreckage, its location very close to the last radar point, and witness statements.

The C_L and airspeed data computed from the radar returns indicate that the flaps must have been deployed at some time prior to 15:44:18, since the required C_L exceeded the C_{Lmax} for flaps up beyond this time, but the airplane continued flying. Consideration of the power requirements computed from the radar data suggests that the flaps may have been deployed to 20° around 15:43:30, shortly after the time the airplane decelerated below the 140 KCAS $V_{FE,20}$ speed.

The roll angle computed from the radar data indicates that N856JT required approximately 13° of roll during the right turn between 15:42:55 and 15:43:50, as the airplane maneuvered to line up with the extended runway centerline. The roll angle required during the final, 360° left turn is about 15° to 25°, with the roll angle increasing from about 5° left to 22° left between 15:44:20 and 15:44:30. This increase in roll angle corresponds to the time that the airplane arrested its deceleration and descent (i.e., decay in energy) and leveled at

approximately 95 KCAS and 1100 ft. MSL. Associated with this level-off is an increase in required horsepower. If the increase in horsepower were only available from one engine (as is suggested by the pilot's reports of an engine problem), then any thrust asymmetry between the two engines would also be increased, and would increase the δ_r and/or β required to compensate for the asymmetry. Consequently, the increase in roll angle at this time may reflect these changing parameters affecting the trim of the airplane.

The increase in required horsepower occurred between 15:44:10 and 15:44:30 as the airplane was leveling off at 1100 ft. MSL, or about 400 ft. AGL. The power increased to about the maximum available from one engine for the corresponding flight conditions. As described above, up until this point the total energy of the airplane was decaying, and the corresponding power requirements were low. At the low power setting, it is possible that any thrust asymmetry between the left and right engines may not have been readily apparent to the pilot through the control or trim of the airplane. Consequently, the pilot may not have become aware of the problem with the left engine until he advanced the power to arrest the energy decay; at that point, the thrust asymmetry would have become apparent in the rudder pedal inputs required to maintain zero β (center the ball) and the control wheel inputs required to offset the roll due to any β that had already built up.

Also, by 15:44:15, the airspeed had already decayed to around 95 KCAS, close to the $V_{MC,20}$ of 93 KCAS. Consequently, with full power on the good engine, at this speed the airplane may have been close to the limit of controllability. The airplane would have been easier to control at lower power settings on the good engine, but may still have presented a challenging situation to the pilot, given the low energy state of the airplane and its proximity to the ground.

During the final left turn, the highest priority to ensure the safety of the flight would have been to increase the control margin by increasing the airspeed further above the 93 KCAS $V_{MC,20}$ speed. However, to increase the speed without changing the configuration of the airplane, the pilot would have had to increase power on the good engine (thereby exacerbating the thrust asymmetry and control problem at low speed, even if additional power were available), trade altitude for airspeed (which the pilot may have been reluctant to do, given that the airplane was only about 400 ft. AGL at the time), or perform some combination of these actions. The pilot could also have increased the speed and margin from $V_{MC,20}$ by retracting the landing gear, thereby lowering the airplane's drag. Nonetheless, at the time the power was increased between 15:44:10 and 15:44:30, the airplane was already in a difficult situation because of the combination of low altitude, low airspeed, and the reported problem with the left engine.

_____

John O'Callaghan
National Resource Specialist - Aircraft Performance
Office of Research and Engineering

F. REFERENCES

1. Federal Aviation Administration, *Aircraft Accident Package: TUL-ATCT-0091, N856JT, MU2.* Accident report dated January 14, 2014.

2. Mitsubishi Heavy Industries America, Inc., *Memorandum to Cassandra Johnson – NTSB, from Ralph Sorrells – MHIA: MU02B data requested via e-mail to Jim Silliman,* memorandum dated December 10, 1998. (MHIA proprietary document).

3. Mitsubishi Heavy Industries, Ltd., Nagoya Aircraft Works, *Engineering Report: Aerodynamic Data for the MU-2 Flight Simulator*, Report # NA-16989, June 3, 1979. (MHI proprietary document).

4. Mitsubishi Heavy Industries, *Flight path analysis #306,* document # YET-14063, February 3, 2014, revised May 15, 2014 (MHI proprietary document).

5. Mitsubishi Heavy Industries, *MU-2B-25 Airplane Flight Manual,* JCAB approved 02-09-72, reissued 03-03-87.

6. National Transportation Safety Board, Office of Aviation Safety, *Witness Records of Conversation.* Various emails from NTSB IIC to NTSB Aircraft Performance Specialist, 3/12/2014 – 4/08/2014.

TABLES

TUL ASR Time, HH:MM:SS CST	Range nmi	Azimuth ACPs	Mode C altitude, feet MSL[1]	Latitude	Longitude	Distance east of KTUL runway 18L, nmi	Distance north of KTUL runway 18L, nmi
15:41:59.25	59.84	3965	3914	N 36° 23' 03.0"	W 095° 56' 19.1"	-2.78	10.20
15:42:03.94	59.48	3978	3814	N 36° 22' 50.3"	W 095° 56' 02.6"	-2.56	9.99
15:42:08.54	59.09	3992	3714	N 36° 22' 38.0"	W 095° 55' 45.6"	-2.33	9.79
15:42:13.16	58.72	4004	3614	N 36° 22' 25.3"	W 095° 55' 31.5"	-2.14	9.57
15:42:17.79	58.34	4019	3414	N 36° 22' 12.5"	W 095° 55' 14.8"	-1.91	9.36
15:42:22.38	57.97	4032	3314	N 36° 22' 00.6"	W 095° 55' 01.0"	-1.73	9.16
15:42:27.07	57.59	4049	3214	N 36° 21' 48.9"	W 095° 54' 43.5"	-1.49	8.97
15:42:31.67	57.22	4062	3014	N 36° 21' 36.5"	W 095° 54' 30.9"	-1.32	8.76
15:42:36.30	56.84	4080	2914	N 36° 21' 25.4"	W 095° 54' 13.8"	-1.09	8.58
15:42:40.92	56.47	4095	2714	N 36° 21' 13.0"	W 095° 54' 00.5"	-0.91	8.37
15:42:45.57	56.11	14	2614	N 36° 21' 02.1"	W 095° 53' 47.6"	-0.74	8.19
15:42:50.19	55.73	31	2514	N 36° 20' 50.2"	W 095° 53' 33.5"	-0.55	7.99
15:42:54.81	55.36	48	2314	N 36° 20' 39.3"	W 095° 53' 19.9"	-0.37	7.81
15:42:59.45	54.98	66	2314	N 36° 20' 27.4"	W 095° 53' 06.2"	-0.18	7.61
15:43:04.06	54.62	84	2214	N 36° 20' 16.4"	W 095° 52' 52.9"	-0.00	7.43
15:43:08.70	54.27	98	2214	N 36° 20' 05.8"	W 095° 52' 43.6"	0.12	7.25
15:43:13.30	53.89	114	2214	N 36° 19' 53.6"	W 095° 52' 33.6"	0.26	7.05
15:43:17.97	53.53	127	2214	N 36° 19' 42.4"	W 095° 52' 26.4"	0.35	6.86
15:43:22.56	53.17	137	2214	N 36° 19' 31.3"	W 095° 52' 22.2"	0.41	6.68
15:43:27.24	52.80	147	2214	N 36° 19' 19.5"	W 095° 52' 18.6"	0.46	6.48
15:43:31.81	52.44	154	2114	N 36° 19' 08.5"	W 095° 52' 17.6"	0.47	6.30
15:43:36.47	52.08	159	2014	N 36° 18' 57.3"	W 095° 52' 18.5"	0.46	6.11
15:43:50.29[2]	*6.09*	*173*	*N/A*	*N 36° 18' 26.4"*	*W 095° 52' 22.1"*	*0.41*	*5.60*
15:43:54.85[2]	*5.94*	*172*	*N/A*	*N 36° 18' 18.1"*	*W 095° 52' 26.8"*	*0.35*	*5.46*
15:43:59.53[2]	*5.78*	*177*	*N/A*	*N 36° 18' 08.2"*	*W 095° 52' 28.0"*	*0.33*	*5.29*
15:44:04.14	51.72	184	1414	N 36° 17' 59.1"	W 095° 52' 27.7"	0.34	5.14
15:44:08.74	51.36	190	1314	N 36° 17' 50.2"	W 095° 52' 28.1"	0.33	4.99
15:44:13.39	51.00	197	1314	N 36° 17' 42.7"	W 095° 52' 27.3"	0.34	4.87
15:44:17.97	50.64	205	1214	N 36° 17' 36.2"	W 095° 52' 25.5"	0.37	4.76

Notes:
1. Mode C altitude shown is recorded pressure altitude plus 314 ft. to account for altimeter setting of 30.26” Hg.
2. Primary return only.

Table 1 (page 1 of 2). TUL ASR returns associated with N856JT. Data is for secondary returns with beacon code 4615, except for the three primary returns noted.

TUL ASR Time, HH:MM:SS CST	Range nmi	Azimuth ACPs	Mode C altitude, feet MSL[1]	Latitude	Longitude	Distance east of KTUL runway 18L, nmi	Distance north of KTUL runway 18L, nmi
15:44:22.58	50.28	214	1114	N 36° 17' 28.9"	W 095° 52' 23.7"	0.39	4.64
15:44:27.20	49.94	224	1114	N 36° 17' 22.0"	W 095° 52' 21.3"	0.42	4.52
15:44:31.85	49.58	239	1114	N 36° 17' 17.3"	W 095° 52' 14.5"	0.52	4.45
15:44:36.53	49.22	255	1114	N 36° 17' 13.8"	W 095° 52' 06.3"	0.63	4.39
15:44:41.14	48.86	267	1114	N 36° 17' 14.2"	W 095° 51' 58.0"	0.74	4.39
15:44:45.72	48.52	277	1114	N 36° 17' 16.5"	W 095° 51' 49.6"	0.85	4.43
15:44:50.35	48.16	279	1114	N 36° 17' 22.7"	W 095° 51' 43.6"	0.93	4.54
15:44:54.98	47.80	278	1114	N 36° 17' 29.2"	W 095° 51' 39.6"	0.98	4.64
15:44:59.60	47.45	271	1114	N 36° 17' 36.2"	W 095° 51' 39.7"	0.98	4.76
15:45:04.17	47.09	261	1114	N 36° 17' 43.4"	W 095° 51' 42.0"	0.95	4.88
15:45:08.81	46.73	251	1114	N 36° 17' 49.1"	W 095° 51' 45.6"	0.90	4.98
15:45:13.36	46.39	238	1114	N 36° 17' 55.0"	W 095° 51' 51.4"	0.83	5.07
15:45:17.99	46.03	226	1114	N 36° 17' 59.4"	W 095° 51' 57.5"	0.74	5.15
15:45:22.55	45.69	208	1114	N 36° 18' 01.9"	W 095° 52' 09.2"	0.59	5.19
15:45:27.17	45.34	197	1114	N 36° 18' 01.5"	W 095° 52' 17.3"	0.48	5.18
15:45:31.75	44.98	188	1214	N 36° 17' 59.5"	W 095° 52' 24.7"	0.38	5.15
15:45:36.41	44.64	189	1114	N 36° 17' 53.7"	W 095° 52' 27.0"	0.35	5.05

Notes:
1. Mode C altitude shown is recorded pressure altitude plus 314 ft. to account for altimeter setting of 30.26” Hg.
2. Primary return only.

Table 1 (page 2 of 2). TUL ASR returns associated with N856JT. Data is for secondary returns with beacon code 4615, except for the three primary returns noted.

QAF ATCBI-6 Time, HH:MM:SS CST	Range nmi	Azimuth ACPs	Mode C altitude, feet MSL[1]	Latitude	Longitude	Distance east of KTUL runway 18L, nmi	Distance north of KTUL runway 18L, nmi
15:41:53.16	24.75	3041	4114	N 36° 23' 22.7"	W 095° 56' 47.4"	-3.16	10.53
15:42:05.11	24.12	3025	3814	N 36° 22' 49.2"	W 095° 55' 57.9"	-2.49	9.97
15:42:17.08	23.62	3010	3514	N 36° 22' 19.0"	W 095° 55' 17.3"	-1.95	9.47
15:42:29.09	23.12	2994	3114	N 36° 21' 48.1"	W 095° 54' 35.7"	-1.39	8.95
15:42:41.03	22.75	2978	2714	N 36° 21' 17.6"	W 095° 54' 02.9"	-0.94	8.45
15:42:53.01	22.38	2962	2414	N 36° 20' 48.3"	W 095° 53' 29.2"	-0.49	7.96
15:43:05.06	22.00	2945	2214	N 36° 20' 18.4"	W 095° 52' 53.5"	-0.01	7.46
15:43:16.97	21.75	2928	2214	N 36° 19' 48.1"	W 095° 52' 26.5"	0.35	6.96
15:43:28.97	21.75	2913	2114	N 36° 19' 18.8"	W 095° 52' 17.8"	0.47	6.47
15:43:41.02	21.88	2899	1914	N 36° 18' 49.6"	W 095° 52' 18.2"	0.46	5.98
15:43:53.05	22.00	2887	1614	N 36° 18' 24.3"	W 095° 52' 18.5"	0.46	5.56
15:44:05.00	22.25	2877	1414	N 36° 18' 00.4"	W 095° 52' 29.0"	0.32	5.16
15:44:17.01	22.38	2868	1214	N 36° 17' 40.4"	W 095° 52' 31.2"	0.29	4.83
15:44:29.01	22.38	2858	1114	N 36° 17' 20.8"	W 095° 52' 23.0"	0.40	4.51
15:44:40.99	22.12	2852	1114	N 36° 17' 14.4"	W 095° 51' 59.8"	0.71	4.40
15:44:53.04	21.88	2855	1114	N 36° 17' 24.9"	W 095° 51' 45.5"	0.91	4.57
15:45:05.14	21.75	2864	1114	N 36° 17' 44.6"	W 095° 51' 43.6"	0.93	4.90
15:45:17.22	21.88	2873	1114	N 36° 17' 59.4"	W 095° 51' 59.8"	0.71	5.15
15:45:29.26	22.12	2878	1114	N 36° 18' 04.7"	W 095° 52' 20.5"	0.43	5.23

Notes:
1. Mode C altitude shown is recorded pressure altitude plus 314 ft. to account for altimeter setting of 30.26” Hg.

Table 2. QAF ATCBI-6 returns associated with N856JT. Data is for secondary returns with beacon code 4615.

Speed description / definition	Value, KCAS
$V_{FO,5}$ (flaps operating, UP to 5°)	175
$V_{FO,20}$ (flaps operating, 5° to 20°)	140
$V_{FE,5}$ (flaps extended, 5°)	175
$V_{FE,20}$ (flaps extended, 20°)	140
V_{LO} (landing gear operating)	160
V_{LE} (landing gear extended)	162
$V_{MC,5}$ (minimum control, flaps 5°)	100
$V_{MC,20}$ (minimum control, flaps 20°)	93

Table 3. Selected MU-2B-25 airspeed limitations, from Reference 5.

FIGURES

CEN14FA046: Mitsubishi MU 2B-25, N856JT, Owasso, OK, 11/10/2013
Plan view of approach to KTUL runway 18L

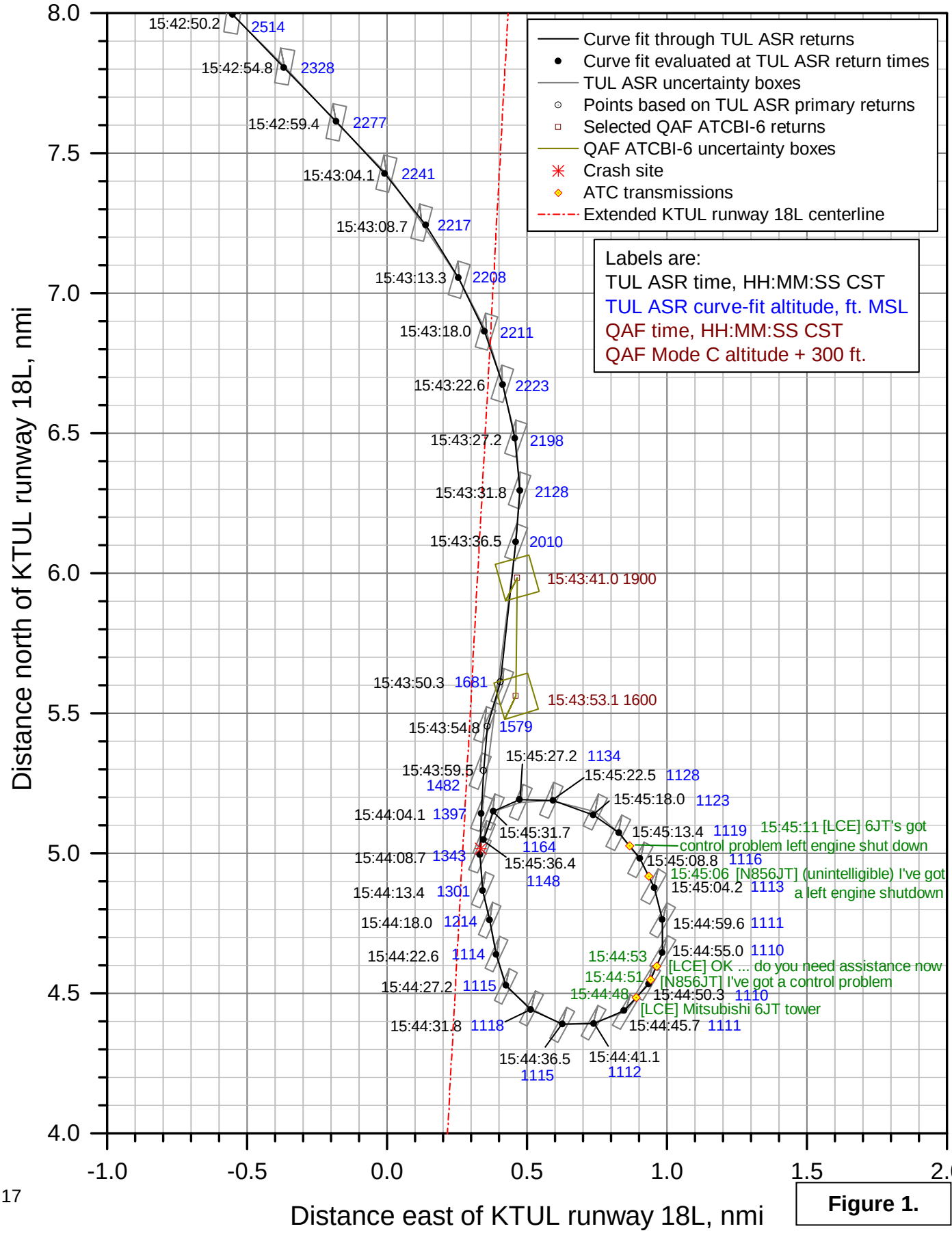

Figure 1.

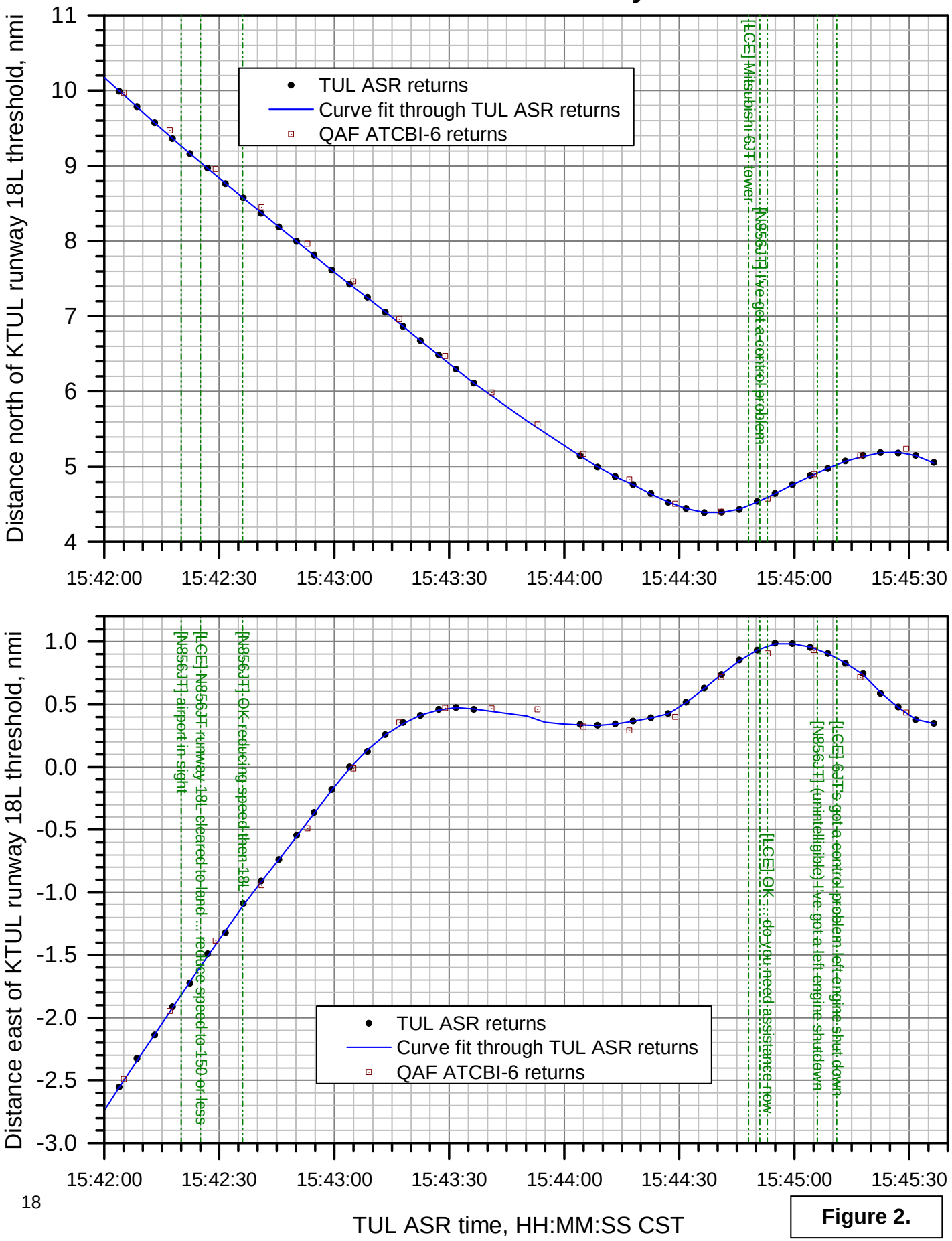
CEN14FA046: Mitsubishi MU 2B-25, N856JT, Owasso, OK, 11/10/2013
Distances north and east of KTUL runway 18L threshold vs. time
Distance north of KTUL runway 18L threshold, nmi
Distance east of KTUL runway 18L threshold, nmi
TUL ASR returns
Curve fit through TUL ASR returns
QAF ATCBI-6 returns
[LCE] Mitsubishi 6JT, tower
[N856JT] I've got a control problem
[LCE] N856JT runway 18L cleared to land ... reduce speed to 150 or less
[N856JT] airport in sight
[N856JT] OK reducing speed then 18L
[LCE] OK ... do you need assistance now
[LCE] 6JT's got a control problem left engine shut down
[N856JT] (unintelligible) I've got a left engine shutdown
15:42:00
15:42:30
15:43:00
15:43:30
15:44:00
15:44:30
15:45:00
15:45:30
TUL ASR time, HH:MM:SS CST

Figure 2.

CEN14FA046: Mitsubishi MU 2B-25, N856JT, Owasso, OK, 11/10/2013
Altitude vs. time from radar returns

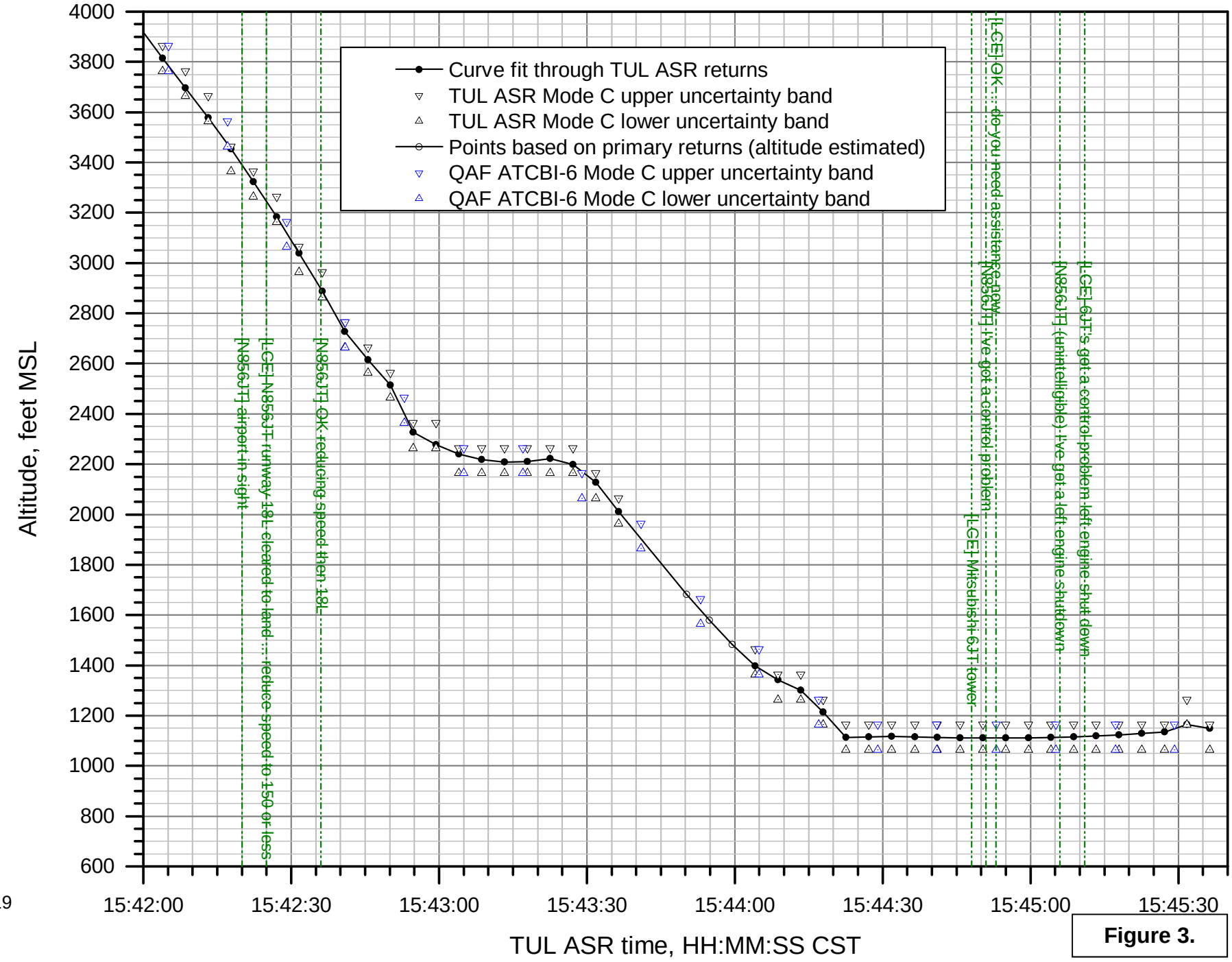

Figure 3.

CEN14FA046: Mitsubishi MU 2B-25, N856JT, Owasso, OK, 11/10/2013
Profile view of approach to KTUL runway 18L

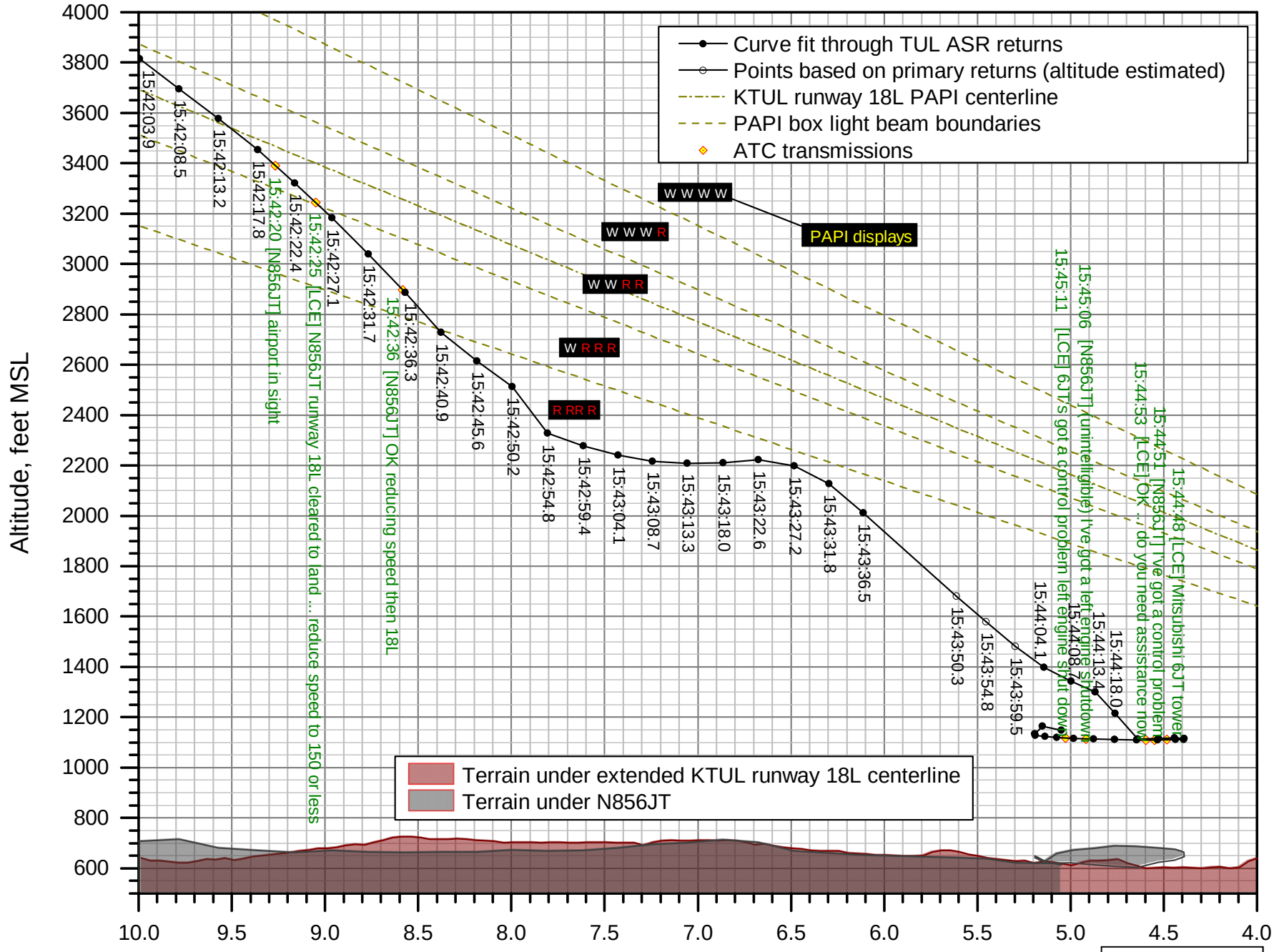

Figure 4.

CEN14FA046: Mitsubishi MU 2B-25, N856JT, Owasso, OK, 11/10/2013
Winds aloft from upper air sounding from KSGF at 18:00 CST on 11/10/2013

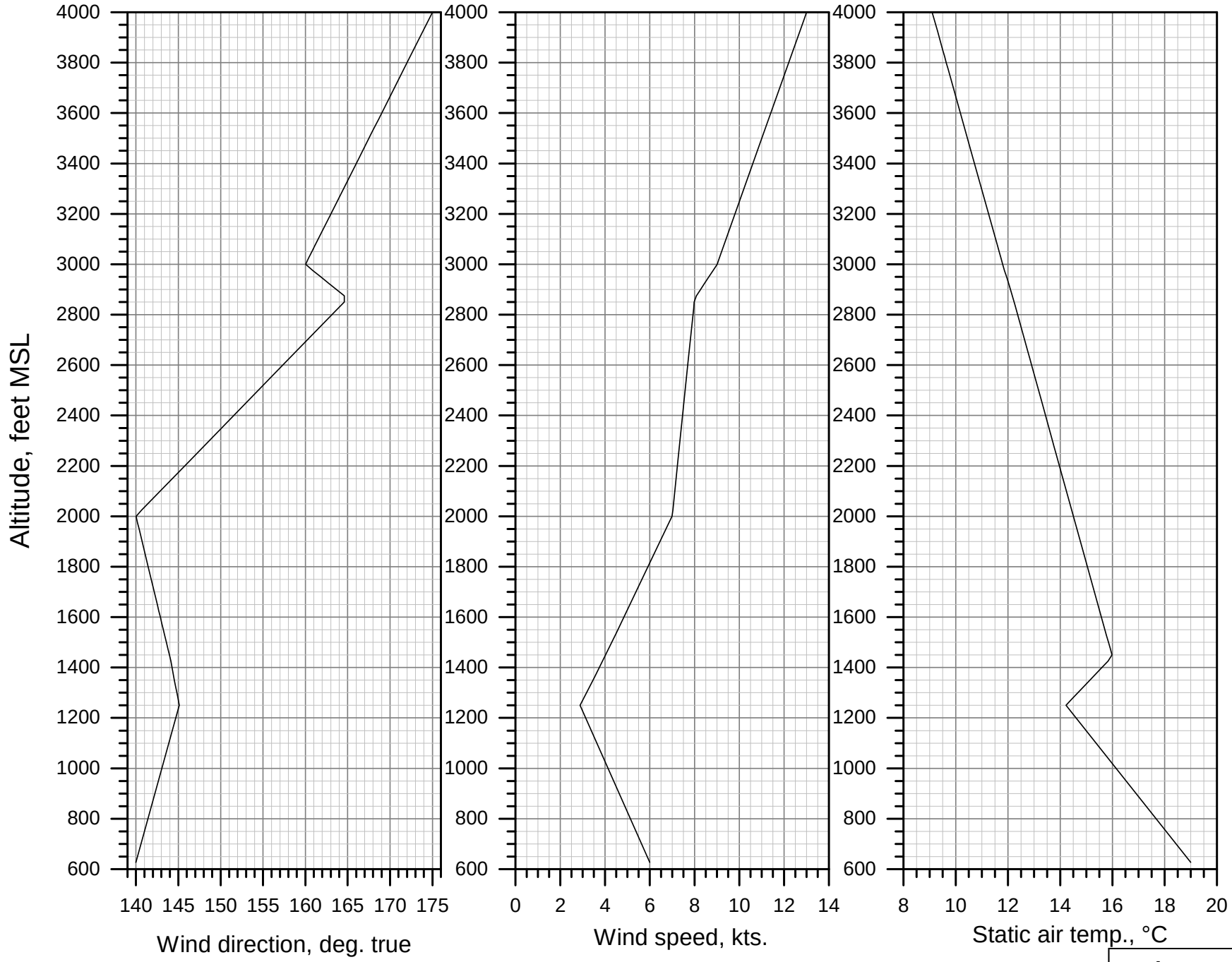

Figure 5.

CEN14FA046: Mitsubishi MU 2B-25, N856JT, Owasso, OK, 11/10/2013
Speeds & rate of climb from curvefit of radar returns

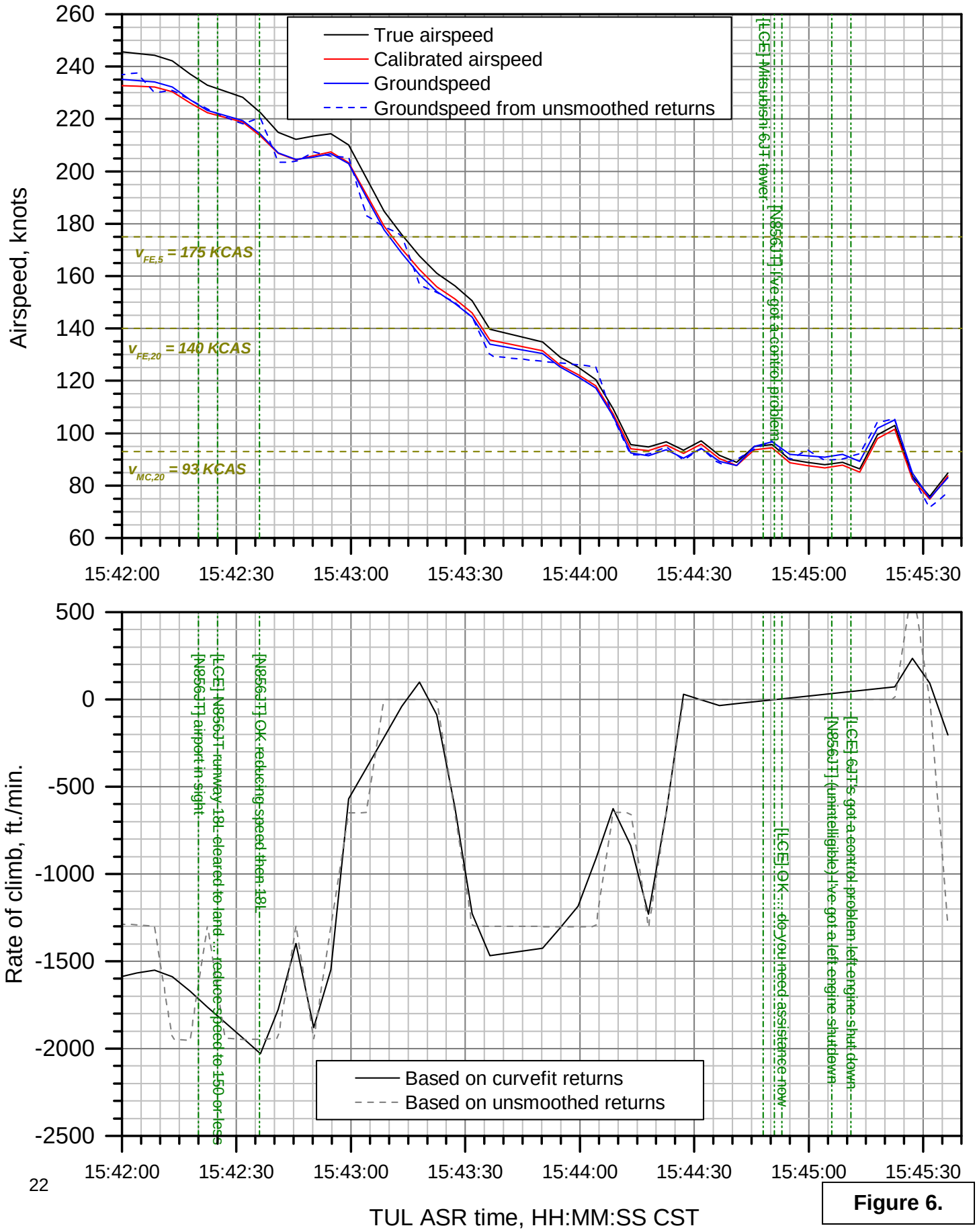

Figure 6.

CEN14FA046: Mitsubishi MU 2B-25, N856JT, Owasso, OK, 11/10/2013

Longitudinal flight angles and C_L from curvefit of radar returns

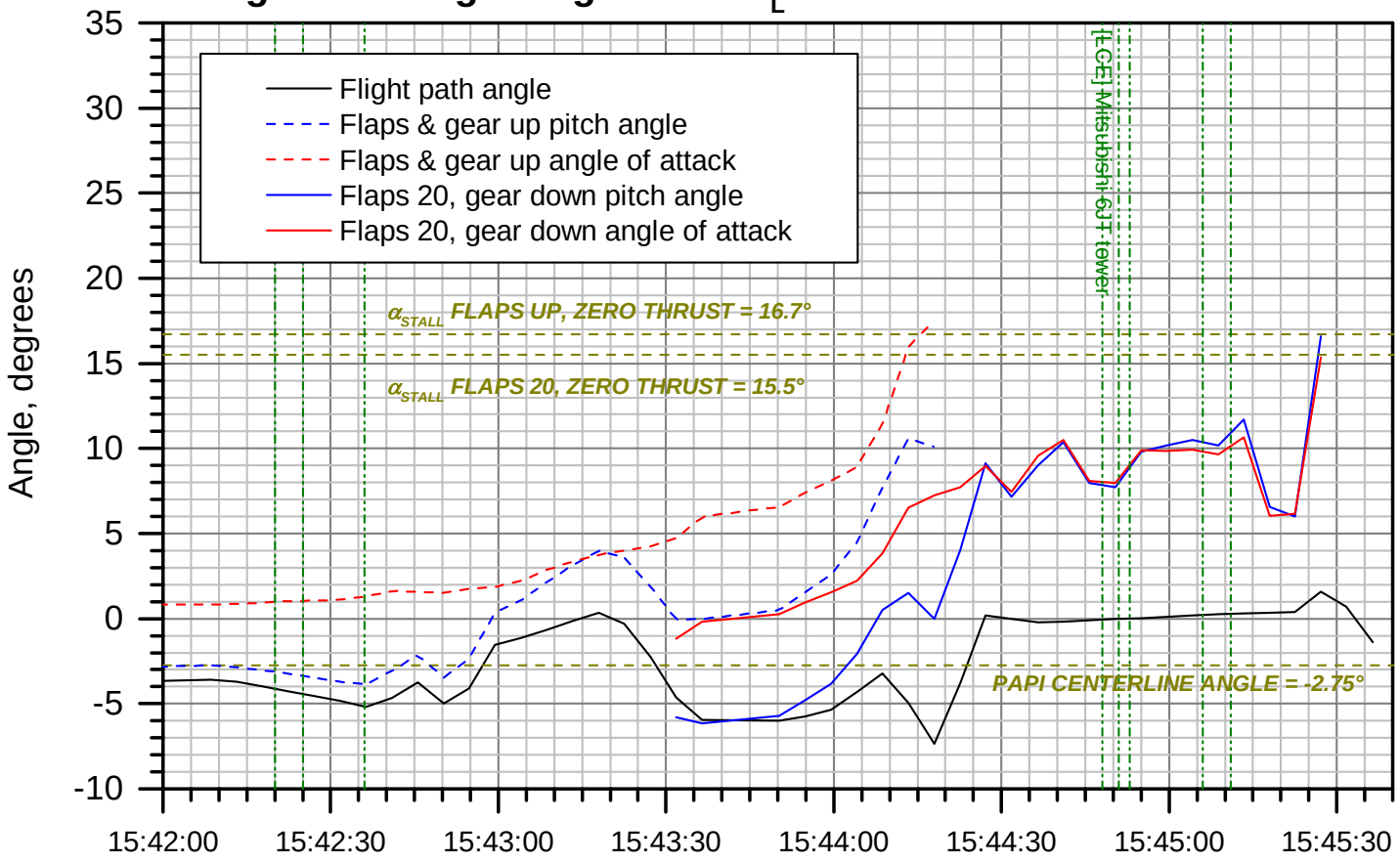

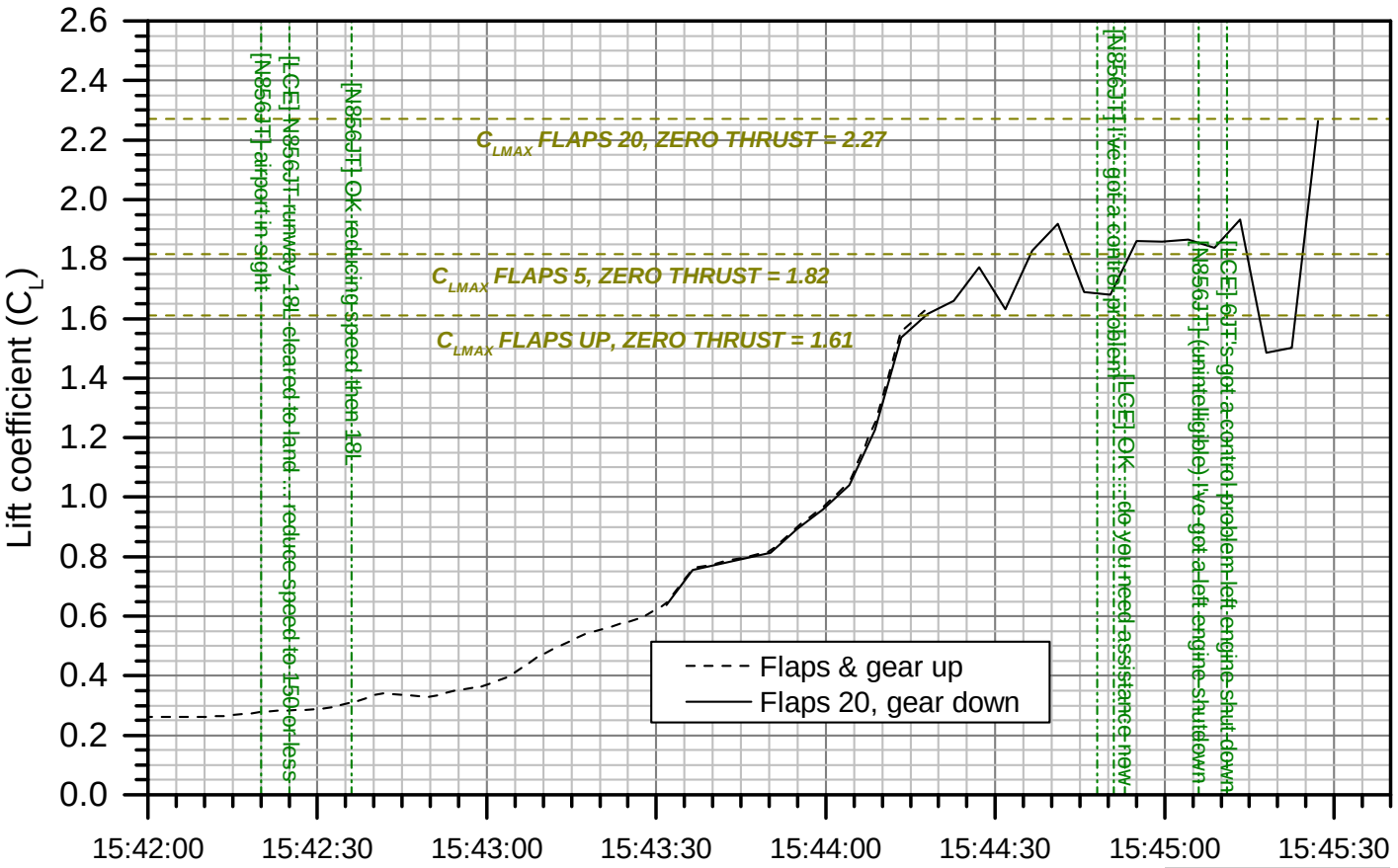

Figure 7.

CEN14FA046: Mitsubishi MU 2B-25, N856JT, Owasso, OK, 11/10/2013
Roll and heading angles from curvefit of radar returns

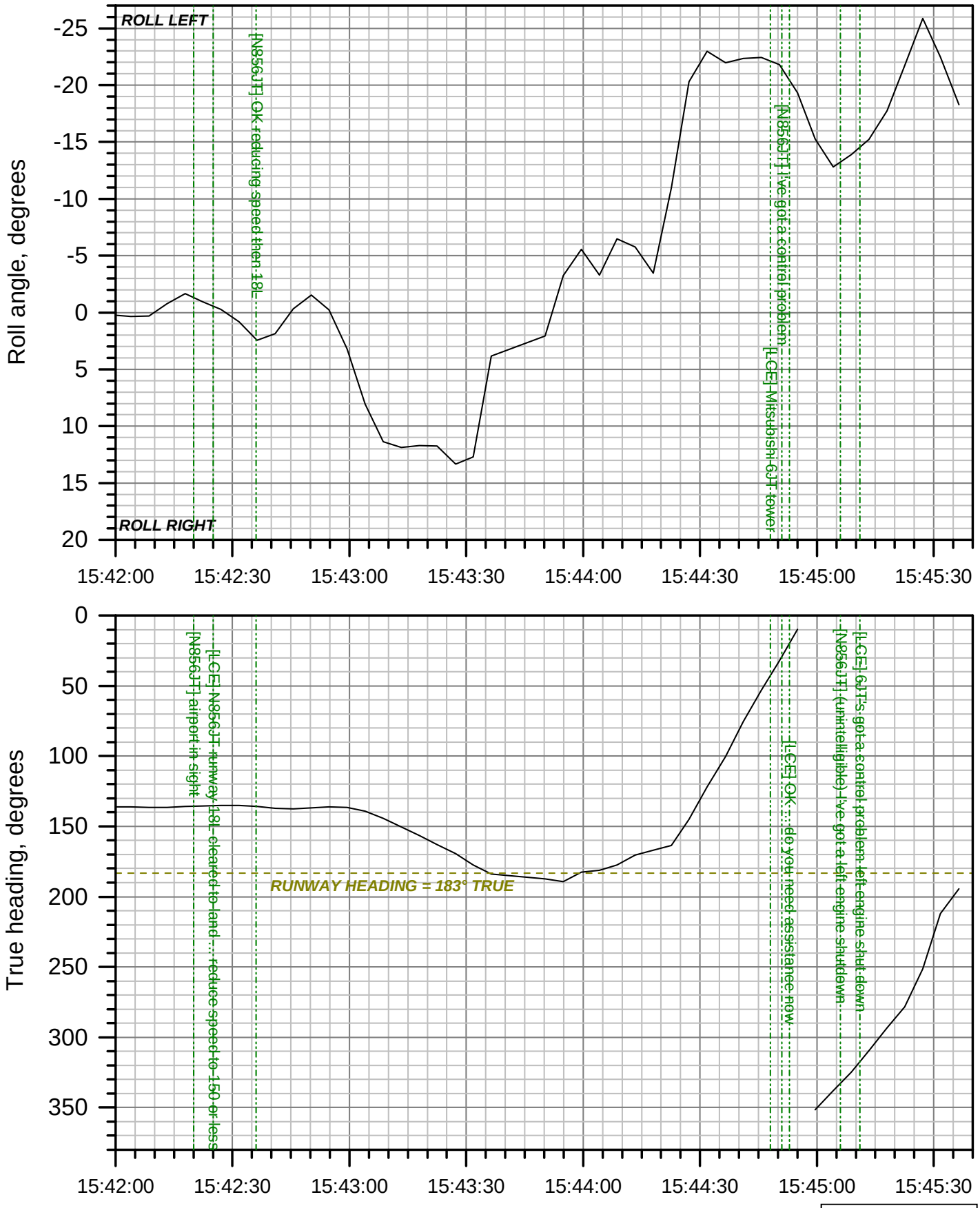

Figure 8.

CEN14FA046: Mitsubishi MU 2B-25, N856JT, Owasso, OK, 11/10/2013

C_D, horsepower and energy from curvefit of radar returns

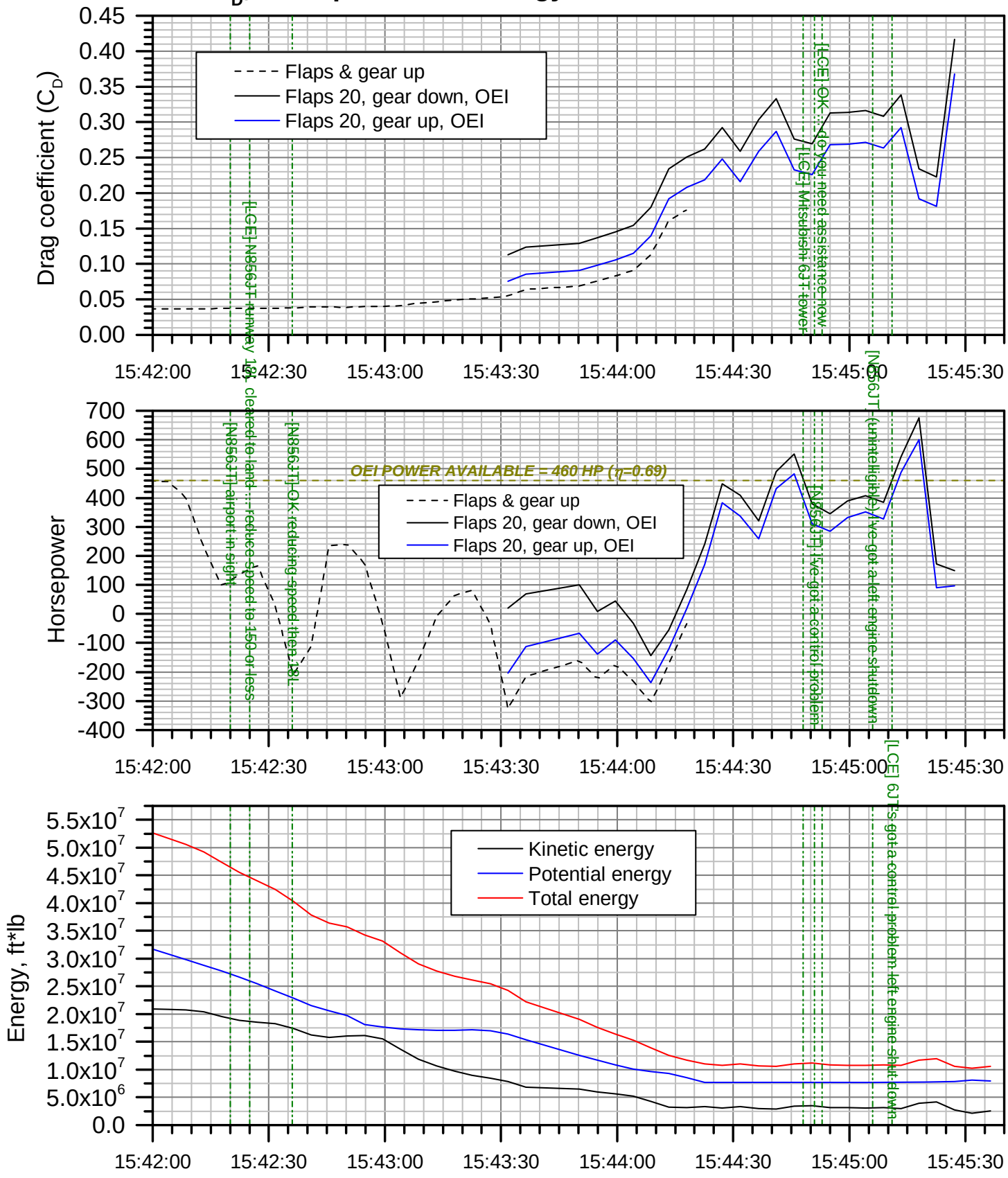

Figure 9.

THIS PAGE INTENTIONALLY LEFT BLANK